Submitted to Journal of
Nuclear Materials

LBL-1131
Preprint ..

THE KINETICS OF ACTINIDE REDISTRIBUTION AND PORE MIGRATION BY VAPOR MIGRATION IN MIXED OXIDE FUELS

Donald R. Olander

August 1972

AEC Contract No. W-7405-eng-48

LBL-1131

DISCLAIMER

THE KINETICS OF ACTINIDE REDISTRIBUTION AND PORE MIGRATION BY VAPOR MIGRATION IN MIXED OXIDE FUELS

By Donald R. Olander

Inorganic Materials Research Division of the Lawrence Berkeley Laboratory and the Department of Nuclear Engineering of the University of California, Berkeley, California 94720, USA

ABSTRACT

The kinetics of vapor migration-driven restructuring and actinide redistribution along continuous cracks or in closed pores was studied analytically. The former was modeled by a rectangular crack with the temperature gradient along the major axis. Redistribution of fuel constituents was considered to occur by molecular diffusion in the gas filling the crack. Hyperstoichiometric U-Pu oxide was treated so that only a single diffusing species (UO_3) needed to be considered, at least in the early stages of the process. The dependence of the kinetics upon oxygen-to-metal ratio, temperature gradient and crack dimensions was investigated for fuel containing 20% plutonium.

Pore migration in mixed oxides differs from the analagous process in pure stoichiometric urania in that the composition as well as the temperature of the two faces of the pore may be different. It was found that pore migration does not lead to actinide redistribution. The velocity of the pores in mixed hyperstoichiometric fuel is $\sim$ 3 times faster than that in pure UO_2.

I. INTRODUCTION

Among the changes in materials properties induced in reactor fuel pins by the steep temperature gradient needed to remove fission heat, restructuring and actinide redistribution have the most profound influence upon thermal performance. Restructuring refers to gross movement of the entire fuel mass from the center towards the periphery, usually accompanied by formation of a central void. Actinide redistribution denotes the unmixing of the heavy metal components of a fuel body initially of uniform composition. Of the various mechanisms that have been proposed to explain these two phenomena, the most important appear to depend upon migration of the heavy metals of the fuel in gas filled spaces within the fuel pin (1-10). The pressures of the oxides of uranium and plutonium are generally higher at the hot central portion of the fuel than at the cooler pellet surface, and the concentration gradient so generated may result in migration of these species via molecular diffusion in the gas.

In order to analyze restructuring and actinide redistribution kinetics by vapor migration, the geometry of the gaseous medium must be specified. Two types of gas-filled voids are considered:

(1) Radial cracks, fissures or interconnected porosity which provide a continuous gas-filled path along the temperature gradient.

(2) Closed pores which accomodate either the porosity of the fabricated fuel or a portion of the fission gases released during irradiation.

The migration processes are strongly dependent upon the composition of the solid fuel. Two fuels are investigated:

(a) Stoichiometric UO_2 used in thermal reactor fuel elements.

(b) Mixed uranium-plutonium oxides used in fast reactor fuel designs.

The migration of pores in pure UO_2 (combination 2a) has been treated by many workers (11-15). Although the existence of closed pores and evidence of their motion up the temperature gradient have been thoroughly documented, the importance of radial cracks and fissures in vapor transport processes has been inferred mainly by the success of the CO_2/CO mechanism proposed by Rand and Markin (16) to explain oxygen redistribution. There is no reason, however, why such gas pathways might not also provide a means of transporting pure species such as UO_2 (combination 1a) or of redistributing the heavy metals (combination 1b). Analysis of an idealized model of these processes is presented here. In addition, pore migration in mixed oxides fuels (combination 2b) is treated.

In order to simplify the analysis of migration along a crack, cartesian geometry rather than the cylindrical geometry of a fuel rod is utilized. Such an idealization streamlines the analysis and avoids having to specify whether a planar crack in a fuel element is oriented perpendicular to or parallel to the rod axis. In addition, the one-dimensional cartesian geometry is applicable to out-of-pile experiments designed to investigate migration phenomena.

II. DIFFUSION-CONTROLLED DISTILLATION OF A PURE COMPONENT IN A CRACK

Figure 1 shows a crack along the length of a piece of fuel which supports a constant temperature gradient in the z-direction. The crack is of width b and length L but is infinite in extent in the direction perpendicular to the drawing. The solid is assumed

to contain many such longitudinal cracks, such that each crack may be associated with a thickness 2H of solid. The ends of the crack at z=0 and z=L are assumed to be closed. No transport is considered to occur within the solid. The crack is assumed to be filled with an inert gas (helium or xenon) at a pressure of $\sim$ 10 atm. Bulk fluid motion due to natural convection driven by temperature inequalities or by the flux of the distilling species is neglected. The latter source of hydrodynamic flow is negligible if the mole fraction of the diffusing species in the inert gas is small, as is the case considered here.

As a result of the temperature gradient in the z-direction, the pressure of the distilling component at the surface of the crack (y=0 and y=b) is given by:

$$p^\circ = A\exp(-\Delta H_v/kT) \qquad (1)$$

where p° is the vapor pressure of the pure species at temperature T, ΔH_v is its heat of vaporization, k is the Boltzmann constant and A is a constant.

The temperature variation along the z-direction is given by:

$$T(z) = T_o - (T_o - T_s)(z/L) \qquad (2)$$

where T_o and T_s are the temperatures at the hot and cold ends, respectively.

Transport of the distilling species is assumed to occur by molecular diffusion in the gas filling the crack. The flux is given by Fick's law as:

$$\underline{J} = -CD\nabla x$$

where $\underline{J}$ is the flux of the diffusing solute, C is the total concentration of the gas phase (assumed ideal) and D is the binary diffusion coefficient of the distilling species in the inert gas. The mole fraction of the solute is denoted by x. Because of the temperature variation along the length of the crack, both C and D vary with z. However, since $C = p_{tot}/kT$ (where p_{tot} is the total pressure of the gas) and D varies approximately as $T^{3/2}$, the product CD is relatively insensitive to temperature. To a first approximation, the temperature dependence of the product CD may be neglected by comparison to the very strong temperature variation of the vapor pressure of the diffusing substance. The flux is then given by:

$$\underline{J} = - \frac{D}{kT} \nabla p \tag{3}$$

where the ratio D/T is assumed constant at the average temperature of the system and p(y,z) is the partial pressure of the solute (equal to xp_{tot}) at location (y,z) in the crack.

At steady state, conservation of the diffusing species requires that:

$$\nabla \cdot \underline{J} = 0 \tag{4}$$

For the rectangular crack of Figure 1, Eqs (3) and (4) may be combined to yield:

$$\frac{\partial^2 p}{\partial y^2} + \frac{\partial^2 p}{\partial z^2} = 0 \tag{5}$$

which is subject to the following boundary conditions:

$$p(0,z) = p(b,z) = p^\circ(z) \tag{6}$$

where $p^\circ(z)$ is a known function of z obtained by combining Eqs (1) and (2). Because the ends of the crack are assumed to be closed, the remaining boundary conditions are:

$$\left(\frac{\partial p}{\partial z}\right)_{z=0} = \left(\frac{\partial p}{\partial z}\right)_{z=L} = 0, \text{ for all } y \qquad (7)$$

Eqs (5) - (7) may be solved by separation of variables (17), but this method was rejected in favor of direct numerical solution. Although the former solution method works satisfactorily for the present problem, it proved unwieldy when applied to mixed oxide fuels. In the latter case, the boundary condition analagous to Eq (6) is time-dependent, and the separation of variables solution was found to be inaccurate, too time consuming even on a large computer, and excessively subject to the usual instabilities attendant to solving partial differential equations numerically. Eqs (5) - (7) were therefore solved by finite difference techniques for the partial pressure profile and the flux at the surface of the crack. It is convenient to express the results in terms of the dimensionless quantities:

$$P = \frac{p}{p^\circ(T_o)} \qquad (8)$$

$$Z = z/L \quad \text{and} \quad Y = y/L \qquad (9)$$

The partial pressure profiles shown in Figure 2 for $b/L = 0.2$, $\Delta H_v = 135.5$ kcal/mole (representing UO_2) and end temperatures of 2500°K and 1000°K are typical of those found for all crack geometries (only b/L was varied).

The rate of transport of the solute down the temperature gradient by the molecular diffusion controlled distillation process

is expressed by the flux normal to the crack surface, which is:

$$J_y = -\frac{D}{kT}\left(\frac{\partial p}{\partial y}\right)_{y=0} = -\frac{Dp^\circ(T_o)}{kTL}\left(\frac{\partial P}{\partial Y}\right)_0 \qquad (10)$$

Figure 2 shows that the wall gradient is negative for $Z<0.04$ and positive for greater distances. Therefore, UO_2 vaporizes from the hot zone and condenses in the cold regions of the crack. The variation of the wall flux with distance along the temperature gradient is shown in Figure 3. The fluxes are positive near the hot end but negative over most of the crack length. The areas between zero abcissa and the positive and negative portions of each curve are equal, since no uranium is lost from the system. The region over which the vaporization and condensation rates are significant is markedly decreased by reduction of the width-to-length ratio of the crack.

A convenient measure of the rate of transport of the pure species down the temperature gradient is the integral of the absolute value of the wall flux over the entire length of the crack, or

$$\int_0^1 \left| \left(\frac{\partial P}{\partial Y}\right)_0 \right| dZ$$

This quantity is shown as a function of b/L in Figure 4. The transport rate becomes very small as b/L is decreased.

Although UO_2 migration down a continuous crack parallel to the temperature gradient does lead to restructuring in the sense that solid is displaced from the hot towards the cold end, the process would soon cease as the cooler regions of the fissure were closed by condensed material. The preceeding analysis was

intended primarily to illustrate the nature of the migration process for a simple case. Vapor migration of fuel constitutents in a mixed oxide, which is treated in the following section, is formulated in a similar manner. However, the boundary condition at the crack surface is related to the U/Pu ratio, which changes with time at each position along the temperature gradient.

III. URANIUM MIGRATION IN MIXED OXIDES

In hyperstoichiometric mixed oxide fuels, the major heavy metal constituent of the gas phase is UO_3. The equilibrium pressure of this species above $U_{0.85}Pu_{0.15}O_{2.05}$ at 2000°K, for example, is more than three orders of magnitude greater than the UO_2 pressure and four orders of magnitude greater than the PuO_2 pressure (16). The preponderance of UO_3 persists as long as the fuel is hyperstoichiometric. In order to restrict the analysis to a single gaseous heavy metal species, only hyperstoichiometric oxides are considered. Extension to hypostoichiometric fuel is straightforward but involves treating the diffusional kinetics of two or more actinide oxides simultaneously.

Thermochemistry of a fuel block which has both non-uniform temperature and uranium profiles

Consider fuel in which the initial uranium and plutonium atom densities of the fuel are N°_U and N°_{Pu}, respectively. The cation fraction of plutonium of the fresh fuel is

$$q_o = \frac{N^\circ_{Pu}}{N^\circ_U + N^\circ_{Pu}} = \frac{\gamma^\circ_{Pu}}{1 + \gamma^\circ_{Pu}} \qquad (11)$$

where

$$\gamma^{\circ}_{Pu} = N^{\circ}_{Pu}/N^{\circ}_{U} \tag{12}$$

is the initial plutonium-to-uranium ratio of the fuel. As a result of the uranium vapor migration process the initially uniform uranium concentration is changed to a distribution in which uranium is depleted in the hot zone and concentrated in the cold zone. The uranium concentration profile after some time under the temperature gradient is denoted by $N_U(z)$. The profile of the cation fraction of plutonium in the fuel corresponding to the non-uniform uranium distribution is

$$q = \frac{N^{\circ}_{Pu}}{N_U + N^{\circ}_{Pu}} = \frac{\gamma^{\circ}_{Pu}}{\gamma_U + \gamma^{\circ}_{Pu}} \tag{13}$$

where

$$\gamma_U = N_U/N^{\circ}_{U} \tag{14}$$

is a dimensionless uranium concentration profile. Because this element is only redistributed within the volume of fuel shown in Figure 1 but is not lost from the system, a total uranium balance requires that:

$$\int_0^1 \gamma_U dZ = 1 \tag{15}$$

In accord with the assumption that PuO_2 is essentially nonvolatile in the time scale required for substantial uranium movement, the Pu concentration at each position is assumed to be independent of time at temperature.

Profiles of the Oxygen Potential and the Uranium Valence

The pressure of molecular oxygen in the gas is assumed to be

controlled by the equilibrium

$$K_C = \frac{p_{CO_2}/p_{CO}}{\sqrt{p_{O_2}}} \tag{16}$$

where K_C is the equilibrium constant of the reaction $CO + \frac{1}{2} O_2 = CO_2$. The pressure of UO_3 is assumed to be small compared to the total carbon pressure (i.e., $p_{CO} + p_{CO_2}$). This assumption uncouples the oxygen redistribution process from the UO_3 diffusion process. That is, the migration of oxygen is due to diffusion of CO_2 and CO but is not affected by the oxygen carried by the diffusing UO_3. This assumption becomes better as the actinide redistribution process proceeds and the UO_3 pressure at the hot end is reduced. At the start of the process, the UO_3 pressure may be comparable to the total carbon pressure at the hot end of the fuel. However, since p_{UO_3} decreases very rapidly with distance down the temperature gradient while total carbon pressure is constant, control of the oxygen potential by the CO_2-CO mixture is but negligibly perturbed by the presence of UO_3 in the vapor. When the above condition is met, CO_2/CO ratio is a function of position along the temperature gradient determined by solution of (18):

$$\frac{2}{p_C K_C}\left[\left(\frac{p_{CO_2}}{p_{CO}}\right)^3 + \left(\frac{p_{CO_2}}{p_{CO}}\right)^2\right] + (1-B)\left(\frac{p_{CO_2}}{p_{CO}}\right) = B \tag{17}$$

where p_C is the total pressure of $CO + CO_2$ in the gas phase and B is a constant to be determined by an oxygen balance.

Oxygen in the gas phase is assumed to be in equilibrium with the fuel at all points along the z-direction. If the constant B

is known, $\Delta\bar{G}_{O_2} = RT\ln p_{O_2}$ is determined at each z by combination of Eqs (16) and (17). According to Rand and Markin (16), the oxygen potential of hyperstoichiometric mixed oxides is a function of temperature and of uranium valence only. Thus, the latter is determined as a function of z once the constant B is specified.

The uranium valence is related to the cation fraction of plutonium and the oxygen-to-total heavy metal ratio by:

$$V_U = 4 + 2\left(\frac{O/M - 2}{1 - q}\right) \tag{18}$$

where the oxygen-to-metal ratio is:

$$O/M = \frac{N_O}{N_U + N^\circ_{Pu}} \tag{19}$$

and N_O is the concentration of oxygen in the solid at position z. Combining Eqs (13), (18), and (19) shows that the oxygen-to-plutonium ratio is given by:

$$\frac{N_O}{N^\circ_{Pu}} = \frac{1}{2}(V_U - 4)\frac{\gamma_U}{\gamma^\circ_{Pu}} + 2\left(\frac{\gamma_U}{\gamma^\circ_{Pu}} + 1\right) \qquad (20)$$

Satisfaction of the oxygen balance requires that the integral of the oxygen concentration over the length of the fuel be equal to the initial amount of oxygen, or:

$$\int_0^1 \frac{N_O}{N^\circ_{Pu}}\, dZ = \left(\frac{O}{M}\right)_o \left(\frac{N^\circ_U + N^\circ_{Pu}}{N^\circ_{Pu}}\right) \qquad (21)$$

where $(O/M)_o$ is the oxygen-to-metal ratio of the fresh fuel. Substitution of Eq (21) into Eq (20) yields:

$$\int_0^1 \left(V_U - 4\right)\gamma_U dZ = 2\left[\left(\frac{O}{M}\right)_o - 2\right]\left(1 + \gamma^\circ_{Pu}\right) \qquad (22)$$

For a given uranium distribution, $\gamma_U(Z)$, the solution proceeds as follows:

1) The constant B is guessed and the oxygen potential is computed as a function of Z by combining Eqs (16) and (17).

2) With $\Delta\bar{G}_{O_2}$ and the temperature known as functions of Z, the profile of uranium valence is determined from the data of Rand and Markin (16).

3) The integral of Eq (22) is performed to verify closure of the oxygen balance. If this restraint is not satisfied, a new value of B is taken and the process is repeated. When the oxygen balance has been satisfied, V_U and $\Delta\bar{G}_{O_2}$ are known as functions of Z.

Equilibrium Pressure of UO_3 at the surface of the Crack

In order to provide the proper boundary condition for diffusion of UO_3 in the gas phase, its equilibrium pressure at the crack sur-

face must be determined. To do this, we first compute the pressure of UO_2 in equilibrium with the fuel whose oxygen potential and uranium valence profiles have just been calculated.

The equilibrium UO_2 pressure at each position is controlled by the reaction:

$$UO_{2+m}(sol'n) = UO_2(g) + \frac{m}{2}O_2(g) \qquad (A)$$

where $m = (2-O/M)/(1-q)$ is related to the local uranium valence by:

$$m = \frac{1}{2}(V_U - 4) \qquad (23)$$

The law of mass action for reaction (A) is:

$$\frac{p_{O_2}^{m/2} \; p_{UO_2}}{1-q} = \exp\left(-\Delta G_A^\circ/RT\right) \qquad (24)$$

where the standard free energy of reaction is given by:

$$\Delta G_A^\circ = -\frac{1}{2}\int_0^m \Delta\bar{G}_{O_2}\, dm' + \Delta G^\circ_{UO_2\ vap} \qquad (25)$$

The last term is the standard free energy of vaporization of UO_2, taken as*:

$$\Delta G^\circ_{UO_2,vap} = 135.5-35.8T \qquad (26)$$

The partial pressure of UO_3 at the crack surface is obtained from the equilibrium of the reaction:

$$UO_2(g) + \frac{1}{2}O_2(g) = UO_3(g) \qquad (B)$$

* In Eq (26) and in the remainder of this paper, standard enthalpies and entropies of reaction are expressed in kcal/mole and eu, respectively. The temperature is in units of 10^3°K.

for which:

$$\frac{p_{UO_3}}{p_{UO_2}\sqrt{p_{O_2}}} = \exp\left(-\Delta G_B^\circ/RT\right) \qquad (27)$$

The standard free energy change for reaction (B) is given by (16):

$$\Delta G_B^\circ = -96.5 + 21.5T \qquad (28)$$

Combining Eqs (23) - (28) and approximating the oxygen potentials reported by Rand and Markin (16) for hyperstoichiometric metal oxides (V_U>4.001) by: $\Delta\bar{G}_{O_2} = -65 + 86(V_U - 4)T$, the pressure of UO_3 at each position at the surface of the crack is given by:

$$p_{UO_3}(0,Z) = p_{UO_3}(b,Z) = \left(\frac{\gamma_U}{\gamma_U + \gamma_{Pu}^\circ}\right) \exp\left\{\left[\frac{1}{2}\left(1-\frac{1}{2}(V_U - 4)\right)\Delta\bar{G}_{O_2} - 16.25(V_U - 4) + 10.75(V_U - 4)^2T - 39.0 + 14.3T\right]\Big/RT\right\} \qquad (29)$$

$V_U(Z)$ and $\Delta G_{O_2}(Z)$ have been determined by the method described in the preceeding section, assuming that the uranium distribution has been specified.

<u>UO_3 Diffusion</u>

The gas phase concentration of UO_3 satisfies Eq (5). The boundary conditions of Eq (7) are valid, but the pressure of UO_3 at the crack surface is given by Eq (29) instead of Eq (6). If the uranium distribution $\gamma_U(Z)$ is known, the flux of UO_3 at the surface of the crack may be determined by the method described earlier for pure UO_2. J_y is given by Eq (10) except that $p^\circ(T_o)$ is replaced by the pressure of UO_3 at Z=0 at the start of the process, $p^*(0,0)$.

The local flux of UO_3 at the crack surface may be related to the local uranium concentration in the solid if two assumptions are

made:

1) Accumulation or depletion or uranium at any particular location does not cause the crack width b to change. Were this feature permitted, the gas diffusion calculation would become intractable.

2) There is no solid state diffusional resistance to uranium transfer to or from the crack surface and the interior of the fuel. This restriction could be relaxed by solving the diffusion equation in the solid in the y-direction. Because of the complexity of solving two coupled partial differential equations, however, this step was not taken. The computations with no solid diffusional resistance in the y-direction lead to more rapid uranium redistribution than full treatment of the crack migration model would show, but the discrepancy decreases as the crack width-to-length ratio decreases.

With these two simplifications, the time rate of change of the uranium concentration at position z may be written as:

$$H\left(\frac{\partial N_U}{\partial t}\right) = -J_y \tag{30}$$

or, in terms of the dimensionless variables previously defined, as:

$$\frac{\partial \gamma_U}{\partial (t/\tau)} = \left(\frac{\partial P}{\partial Y}\right)_0 \tag{31}$$

where P is the UO_3 partial pressure divided by the value at Z=0 and t=0, and τ is a characteristic time:

$$\tau = \frac{kTN_U^\circ H^2}{Dp^*(0,0)}\left(\frac{L}{H}\right) \tag{32}$$

Eqs (5) and (31), subject to the boundary conditions of Eq (7) and (29), have been solved numerically for various values of the

parameters b/L, $(O/M)_o$ and T_s. A flow chart of the computation is shown in Figure 5. At each time step, the profiles of $\Delta\bar{G}_{O_2}$ and V_U are recomputed in order to determine the change in the UO_3 pressure at the crack surface according to Eq (29). The change in the uranium concentration of the solid at each position along the temperature gradient is calculated by use of Eq (31).

The Quasi-Equilibrium Uranium Distribution

Uranium transport in the gas phase ceases when the UO_3 pressure at the crack surface is constant over the entire length of the fuel piece. The uranium distribution in the solid for which this is true, $\gamma_U^{eq}(Z)$, may be determined as follows.

The uniform UO_3 pressure attained when uranium transport stops must be very close to that for pure hyperstoichiometric urania at the cold end temperature. In order to reduce the UO_3 pressure over the hotter regions of the fuel to this value, essentially all of the uranium must be removed from the high temperature region of the fuel and transported to the cold end. $\gamma_U^{eq}(Z)$ is very close to zero except as $Z \to 1$, where it rises very sharply to a large value at the cold end. Therefore, we make the assumption that over the range where γ_U^{eq} is rising rapidly from near zero, the uranium valence is approximately constant (this assumption may be verified after the equilibrium solution has been found).

With this assumption, (V_U-4) may be removed from the integral on the left of Eq (22), and taking account of Eq (15), the uranium valence at the cold end is found to be:

$$\lim_{Z\to 1}(V_U-4) = 2\left[(O/M)_o - 2\right](1 + \gamma^{\circ}_{Pu}) \qquad (33)$$

Since the temperature and the uranium valence at the cold end are known, the oxygen potential at Z=1 may be determined from Rand and Markin's data (16). Eq (16), with K_C evaluated at T_s, determines the CO_2/CO ratio at Z=1 and Eq (17) determined the constant B. Since this constant applies to all Z, the CO_2/CO ratio at all positions along the temperature gradient may be computed from Eq (17), and use of Eq (16) at all positions along the temperature gradient determines the oxygen potential profile. The Rand-Markin data then permit the distribution of the uranium valence with Z to be found.

The uniform UO_3 pressure is related to the uranium distribution by Eq (29), in which the exponential term is known from the discussion in the preceding paragraph. Specifically, we may write:

$$p^{eq}_{UO_3} = \left[\frac{\gamma_U^{eq}(Z)}{\gamma_U^{eq}(Z)+\gamma^{\circ}_{Pu}} \right] f(Z) \qquad (34)$$

where, if we take the approximation to $\Delta\bar{G}_{O_2}$ used in deriving Eq (29), f(Z) may be written as:

$$f(Z) = \exp\left[\frac{C_2}{R} - \frac{C_1}{RT} \right] \qquad (35)$$

where

$$C_1 = 32.5\left[1-\tfrac{1}{2}\ (V_U-4)\right] + 16.25(V_U-4) + 39.0$$

$$C_2 = 43\left[1-\tfrac{1}{2}\ (V_U-4)\right](V_U-4) + 10.75(V_U-4)^2 + 14.3 \qquad (36)$$

C_1 and C_2 are taken as constants with the uranium valence given by Eq (33).

Because the uranium concentration is appreciable only very close to Z=1, the reciprocal of temperature distribution in Eq (35) may be expanded in a Taylor series about Z=1 and f(Z) written as:

$$f(Z) = f(1)e^{r(1-Z)} \tag{36}$$

where

$$r = \frac{C_1}{RT_s}\left(\frac{T_o - T_s}{T_s}\right) \tag{37}$$

and f(1) is the value of f at T_s.

Using Eqs (36) in Eq (34) and solving for the equilibrium uranium distribution yields:

$$\gamma_U^{eq}(Z) = \frac{\gamma_{Pu}^{\circ}\, p_{UO_3}^{eq}}{f(1)e^{r(1-Z)} - p_{UO_3}^{eq}} \tag{38}$$

The constant UO_3 pressure is determined by the uranium balance of Eq (15):

$$\gamma_{Pu}^{\circ}\int_0^1 \frac{dZ}{\left[\frac{f(1)}{p_{UO_3}^{eq}}\right]e^{r(1-Z)} - 1} = 1 \tag{39}$$

Eq (39) determines the ratio $f(1)/p_{UO_3}^{eq}$ for the known values of γ_{Pu}° and r. Once this ratio has been determined, the equilibrium uranium distribution may be computed from Eq (38).

The distribution $\gamma_U^{eq}(Z)$ has been termed "quasi-equilibrium" because it does not represent a state of true thermodynamic equilibrium. Rather, it is the uranium distribution at which uranium transport in the gas vanishes, provided that the plutonium in the solid has not migrated at all. However, given sufficient

time, the plutonium will also migrate from the hot end to the cold end. Since at the state of quasi-equilibrium of the uranium, the hot end is practically pure PuO_2, the migration of the latter is identical to the analysis of the transport of a pure species down the crack presented earlier. This process proceeds until the crack is completely filled with solid and no path for further gas phase transport remains. Because the equilibrium pressures of PuO_2 are several orders of magnitude smaller than those of UO_3, the gas phase migration of the plutonium is very much slower than that of UO_3. Consequently, substantial uranium redistribution may occur before appreciable quantities of plutonium have distilled down the crack. In principle, however, the quasi-equilibrium uranium distribution given by Eq (38) is valid only when the plutonium is absolutely non-volatile.

Uranium Redistribution Results

Figures 6-10 depict the progress of actinide redistribution by UO_3 diffusion in a gas filled crack. The conditions for the computation were:

cation fraction of plutonium in fuel = 0.2
initial oxygen-to-metal ratio = 2.05
end temperatures = 2500°K and 1000°K, respectively
total carbon pressure = 1 atm.
crack width-to-length ratio = 0.1

Figure 6 shows the progressive changes in the partial pressure of UO_3 at the crack surface as redistribution occurs. The initial state, denoted by dimensionless time $t/\tau = 0$, represents the condition of the fuel after oxygen redistribution has occurred but before uranium migration has begun. The normalizing factor, $p^*(0,0)$,

is the pressure of UO_3 over the hottest part of the fuel at the start of the uranium transport process. The initial fuel composition and the hot end temperature are $U_{0.8}Pu_{0.2}O_{2.093}$ at 2500°K, respectively, and the corresponding equilibrium UO_3 pressure is 0.068 atm.

The distinguishing features of the curves in Figure 6 are the plateaus at the hot end which develop early in redistribution as a result of the UO_3 vaporization process. At values of the dimensionless times greater than 10 (which is the largest shown in Figure 6), the flat portion of the curve would be lower and extend further into the cooler regions of the fuel than those shown for shorter times. If no plutonium vaporization occurred, the quasi-equilibrium state would be attained when the UO_3 pressure throughout the crack had attained a value of 4×10^{-12} atm. However, long before the quasi-equilibrium state is attained, PuO_2 vapor migration would have become significant. The dashed lines in Figure 6 show the profiles of the PuO_2 pressure over the fuel at the same dimensionless times for which the UO_3 surface pressures were plotted. The PuO_2 pressures increase as redistribution proceeds because the vaporization of UO_3 from the hot zone continually increases the plutonium content of the solid in this region. The UO_3 pressure plateau becomes comparable to the PuO_2 pressures at dimensionless times between 100 and 1000. The calculations would not be valid beyond this point because plutonium vapor migration has not been included in the model. However, a very substantial portion of the total uranium transport occurs before this limit is reached.

Figure 7 shows the distribution of the gradient of the UO_3 pressure at the surface of the crack (which is proportional to the flux from the solid) as a function of distance along the temperature gradient for the same three values of the dimensionless time that were utilized in Figure 6. Initially, the profile of the flux of UO_3 is similar to that for pure UO_2 shown in Figure 2 (except in magnitude) because the pressure of UO_3 has approximately the same temperature dependence as the vapor pressure of a pure material. The flux is quite large near Z = 0, which means that the hot region rapidly becomes deficient in uranium. This loss of uranium from the solid reduces the equilibrium pressure, thereby creating the plateaus seen in Figure 6.

The plateaus of the UO_3 surface pressure at the hot end of the fuel drastically reduce the rate of uranium vaporization from this zone, since the gradient of the UO_3 pressure in the gas along the temperature gradient is removed when the surface pressure is constant. Figure 7 shows that the UO_3 vaporization rate peaks sharply at a point corresponding to the end of the plateau in Figure 6, where the UO_3 surface pressure starts to drop precipitously. The flux profiles in Figure 7 have the appearance of a wave proceeding from the hot end to the cold end. The amplitude of the wave decreases with increasing time because the driving pressure of UO_3 is reduced as the cooler regions of the fuel are encountered. The integral of the flux over the entire length of the fuel is zero, since no uranium is lost in the redistribution process.

Figure 8 shows the evolution of the plutonium content of the solid during redistribution. The advancing waves shown in Figure 7

leave behind them a region of high plutonium concentration, but the condensing uranium depresses the Pu/U ratio ahead of the waves. The quasi-equilibrium distribution is shown on the right of Figure 8. The fuel is essentially pure PuO_2 over 90% of its length and practically pure hyperstoichiometric urania at the cold end. These computations should be viewed as qualitative since the plutonium-uranium ratios are well beyond the range to which the thermochemical data of Rand and Markin apply (16).

Figures 9 and 10 show the distribution of the oxygen potential, uranium valence and the CO_2/CO ratio during redistribution of uranium. Over the range of dimensionless times utilized in Figures 6-8, these distributions change relatively little. The reason for this insensitivity is that the uranium distribution, $\gamma_U(Z)$, enters the oxygen balance only in the integral of Eq (22). As the uranium distribution is shifted towards the cold end, Figure 9 shows that a small increase in the V_U vs Z curve is sufficient to maintain the oxygen balance. The extreme uranium redistribution at quasi-equilibrium, however, causes significant changes in the distributions of Figures 9 and 10.

A convenient measure of the extent of uranium redistribution is the integral of the absolute value of the deviation of the uranium concentration profile from its initial value, which is given by:

$$E(t/\tau) = \begin{matrix}\text{extent of} \\ \text{uranium} \\ \text{redistribution}\end{matrix} = \int_0^1 \left| \gamma_U(Z) - 1 \right| dZ \qquad (40)$$

This quantity is plotted as a function of dimensionless time for the four different sets of input parameters listed in Table 1.

The detailed results shown in Figures 6-10 applied to combination A of Table 1, but the general shapes of the plots are the same for all combinations studied. The redistribution process cannot be characterized by a single time constant. As shown in Figure 11, the rate of redistribution, as measured by Eq (40), continually decreases with increasing time. This behavior reflects the penetration of the flux waves of Figure 7 into regions of fuel at progressively lower temperature.

In order to obtain a numerical estimate of the time required for the redistribution process, the extent of redistribution has been fitted to the function:

$$E(t/\tau) = E(\infty)\left[1 - e^{-\lambda (t/\tau)}\right] \qquad (41)$$

The extent of redistribution determined from the quasi-equilibrium uranium distributions ($E(\infty)$) are shown as the dashed lines in Figure 11. The curves on Figure 11 cannot be fitted to Eq (41) over the entire range of the dimensionless times investigated. However, characteristic rates can be obtained by fitting the curves to Eq (41) at a common dimensionless time, which has been chosen as $t/\tau = 15$. The "half-life" of the redistribution process may then be taken as:

$$t_{1/2} = 0.693\tau/\lambda \qquad (42)$$

Values of τ have been calculated according to Eq (32) in which the diffusion coefficient of UO_3 in Xe at 10 atm total pressure and 2000°K was estimated from kinetic theory (14,19) as ~ 0.2 cm^2/sec. The length of the fuel piece was chosen as 0.2 cm to yield a temperature gradient typical of fast reactor fuel

pins. The crack spacing in the fuel piece was assumed to be equal to the crack length. It is unlikely that in an actual temperature gradient experiment or in an operating fuel rod that the cracks would be any closer together than this, and if they were further apart, the resistance due to diffusion of uranium in the solid in the y-direction would become significant. Table 1 shows that the values of τ calculated by Eq (32) are somewhat over 2 hours for fuel of initial O/M of 2.05 and nearly 10 hours for an O/M of 2.02.

As a result of fitting the curves of Figure 11 at $t/\tau = 15$ to Eq (41) and determining the value of λ for each, the half lives shown in the last column of Table 1 were obtained. These figures approximately represent the time required for the extent of redistribution to change by a factor of e from the value at $t/\tau = 15$, which represents a real time of 35 to 140 hours depending upon the value of the normalizing UO_3 pressure. Based upon this measure, the redistribution of fuel with the lowest O/M is the slowest, which reflects the low UO_3 driving pressures in this material. The fuel with the highest cold end temperature (combination D) is redistributed at the greatest rate. The extent of redistribution of the fuel piece with the narrowest crack (combination B) has the smallest extent of redistribution at a dimensionless time of 15 but the half life listed in Table 1 shows that redistribution is still occurring at an appreciable rate.

The redistribution curves in Figure 8 are similar in shape to the measured plutonium profiles in fuel pins or out-of-file experiments presented by several authors (1, 5, 9). They are also similar to the profiles calculated from the thermal diffusion

mechanism (20). The shape of the distribution, however, is not a useful means of assessing the validity of the model, since any process which conserves total uranium must produce distributions which are above the initial uniform value over part of the fuel and below it over the remaining portion. Although the direction of the redistribution process is correctly predicted by the present calculation, the large plutonium enrichments at the hot end indicated by the model are not observed in the stoichiometric or hypostoichiometric oxides utilized in the experiments. In addition, three simplifications inherent in the model may account for excessively large plutonium concentrations at the hot end.

First, in a reactor fuel pin, UO_3 migration undoubtedly occurs along the axis of the rod due to the axial temperature gradient in the central void. Thus the plane at Z=0 need not be characterized by zero UO_3 flux, as has been assumed in the calculation. Rather, UO_3 may be added to the crack at this point if the pellet is not at the position of peak axial power, or uranium may preferentially migrate away from the pellet via the central void if the pellet is the hottest one in the fuel stack.

Secondly, the fissures through which gas migration occurs may not be as wide or as closely spaced as the values chosen for the sample calculations. If the thickness of fuel associated with each crack is large, reduction of uranium vaporization to or condensation from the gas phase will result from the requirement of transporting uranium to or from the crack surface through the solid. Such a resistance, if significant, would tend to reduce the extent of redistribution at a particular time.

Finally, the purely diffusional model presented here assumes the crack width to remain the same throughout redistribution but does not specify any mechanism by which this may be accomplished. Clearly, the first mechanical effect of uranium transport is to swell the fuel where the vapor condenses and to contract it where UO_3 evaporation has occurred, which would result in closure of the crack in the region of maximum UO_3 condensation. The change in volume of the solid in response to removal or addition of uranium is due to the approximate constancy of the total density of heavy metal atoms at all positions in the fuel. Variations of total density due to thermal expansion, non-uniform Pu/U ratio, or fuel porosity are secondary influences.

The only way that the vapor migration process can continue is for healed cracks to be reopened, or new ones formed, by mechanical stresses acting on the fuel body. If at the same time the total heavy metal concentration of the fuel is to remain constant at all points along the temperature gradient, the forces in the solid which maintain the crack population must also act to move as much of solid material back towards the hot zone as rapidly as vapor migration brings uranium to the cold zone. This mechanical feature of the process may be modeled by assigning a z-direction flow velocity, $v_s(z,t)$, to the solid, the value of which is governed by the requirement of position-independent total heavy metal atom density. A balance on U + Pu in the solid in a differential slice in the z-direction of Figure 1 shows that for constant atom density, that:

$$\frac{\partial v_s}{\partial z} = - \frac{J_v}{(N_U^\circ + N_{Pu}^\circ)H} \qquad (43)$$

where J_y is the flux of UO_3 from the crack surface and $N_U^\circ + N_{Pu}^\circ$ is the total atom density of the heavy metals. Both J_y and v_s are positive in the directions of positive y and z, respectively, in Figure 1. Since $v_s(0,t) = 0$, Eq (43) may be integrated to yield:

$$v_s(z,t) = - \frac{1}{(N_{Pu}^\circ + N_U^\circ)H} \int_0^z J_y(z',t)dz' \qquad (44)$$

The velocity v_s is always negative, which indicates that the solid is relocated towards the hot end during uranium transfer. The maximum value of the solid velocity occurs at the positions in Figure 7 where the flux crosses zero. Eq (44) automatically satisfies the condition at the cold end [$v_s(L,t) = 0$] since the integral of the vapor flux normal to the crack surface over the entire length of the fuel piece is zero.

The presence of bulk motion in the solid implies that the time rate of change of the uranium concentration in the solid is not given correctly by the simple formula, Eq (30). The proper balance on uranium in the solid is:

$$\frac{\partial N_U}{\partial t} + \frac{\partial}{\partial z}(v_s N_U) = - \frac{J_y}{H} \qquad (45)$$

Combining Eqs (44) and (45) and using the dimensionless parameters defined previously yields the following expression for the time rate of change of the uranium content of the solid:

$$\frac{\partial \gamma_U}{\partial (t/\tau)} = \left(\frac{\partial P}{\partial Y}\right)_0 - \frac{1}{1 + \gamma_{Pu}^\circ} \frac{\partial}{\partial Z}\left[\gamma_U \int_0^Z \left(\frac{\partial P}{\partial Y}\right)_0 dZ'\right] \qquad (46)$$

Incorporation of Eq (46) into the model in place of Eq (31) would alter the shape and reduce the rate of advance of the flux waves of Figure 7 but the general features of the redistribution kinetics would remain.

IV. PORE MIGRATION IN MIXED OXIDES

Figure 12 shows a lenticular pore moving in a mixed oxide fuel body. The pore is idealized as a slab of width ℓ but infinite in extent in the plane perpendicular to the direction of the temperature gradient. The temperature increases from left to right in the drawing. The pore moves with a velocity v_p up the temperature gradient. It is assumed that the material ahead of the pore has a cation fraction of plutonium denoted by q_o and an oxygen-to-metal ratio of $(O/M)_o$. We seek to determine:
(a) the composition of the solid behind the moving pore and
(b) the pore migration velocity.

The first question may be answered by considering a material balance over the volume element delineated by the lines marked 1 and 3 in Figure 12. Position 1 is just upstream of the pore in virgin fuel. Position 3 is just behind the boundary of the pore at the cold side. Let the volume element contained within planes at 1 and 3 move with the velocity of the migrating pore. The material balance requires that the rate and composition of the solid moving into the volume element across plane 1 be equal to that leaving the volume element at plane 3. Therefore, a gas-filled pore sweeping through a solid mixture under the influence of a temperature gradient does not produce unmixing of the fuel con-

stituents*.

Consider next a material balance over the volume element defined by the planes at positions 1 and 2 in Figure 12. The latter location is within the gas space of the pore. Assume that the fuel is hyperstoichiometric mixed oxide and that all uranium is transported by molecular diffusion of UO_3 from the hot side to the cold side of the pore. Let the flux of UO_3 in the gas be denoted by J_{UO_3}, which is positive in the direction of the arrow on Figure 12. Similarly, plutonium is transported across the pore by diffusion of PuO_2 in the gas at a rate J_{PuO_2}. Material balances for U and Pu over the volume element between planes 1 and 2 require that $J_{UO_3} = v_p N_U^\circ$ and $J_{PuO_2} = v_p N_{Pu}^\circ$, where N_U° and N_{Pu}° are the uranium and plutonium concentrations of the virgin fuel, respectively. Thus the fractional contribution of plutonium to the total heavy metal diffusion flux is equal to the fraction of plutonium in the fresh fuel, or:

$$\frac{J_{PuO_2}}{J_{UO_3} + J_{PuO_2}} = \frac{N_{Pu}^\circ}{N_U^\circ + N_{Pu}^\circ} = q_o \qquad (47)$$

The following assumptions concerning the gas phase in the pore are made:

(1) Transport in the gas occurs by steady state molecular diffusion.

* The basic difference between zone refining of a solid (21) and a pore moving in a solid mixture is the density of the zone (or pore). In the former case, the liquid zone has a non-zero capacity for accumulating the impurity, since the liquid and solid densities are approximately equal. In pore migration, however, the gas in the pore has a negligible capacity for storing either of the actinides.

(2) The species in the pore consist of an inert gas, CO_2 and CO (total pressure p_C), O_2 and the above mentioned actinide oxides. The partial pressures of these constituents are ordered as follows:

$$p_{Inert} >> p_C$$

$$p_C >> p_{O_2},\ p_{UO_3},\ p_{PuO_2}$$

The first inequality insures that the diffusing species are sufficiently diluted in the inert gas so that their fluxes are given by Eq (3). The second inequality implies that the CO_2/CO ratio in the gas is constant across the pore.

(3) The pore width ℓ is small enough such that differences in all temperature dependent properties of the fuel across the pore may be approximated by one term Taylor series expansions.

The fluxes of the actinide oxides may be written as:

$$J_{UO_3} = \frac{D}{kT\ell}\left[(p_{UO_3})_{hot} - (p_{UO_3})_{cold}\right] \quad (48a)$$

$$J_{PuO_2} = \frac{D}{kT\ell}\left[(p_{PuO_2})_{hot} - (p_{PuO_2})_{cold}\right] \quad (48b)$$

where T is the average temperature at the location of the pore and D is the diffusion coefficient of the actinide oxides in the inert gas (the diffusivities of UO_3 and PuO_2 are assumed equal).

The partial pressures of UO_3 and PuO_2 are assumed to be in equilibrium with the solid at both sides of the pore. Therefore, p_{UO_3} at either surface may be expressed in the form of Eq (34), or by:

$$p_{UO_3} = (1 - q)f \quad (49)$$

where f is given by Eqs (35) and (36). The driving force in Eq (48a) may be written as:

$$(p_{UO_3})_{hot} - (p_{UO_3})_{cold} = (1 - q_{hot})f_{hot} - (1 - q_o)f_{cold} \quad (50)$$

where plutonium fraction at the cold side of the pore has been set equal to the value for the virgin fuel, as indicated previously. Expanding the function f in a Taylor series:

$$f_{hot} = f_{cold} + f'\nabla T\ell \quad (51)$$

where $f' = df/dT$ and ∇T is the temperature gradient. Similarly, the plutonium fraction at the hot side of the pore is given by:

$$q_{hot} = q_o + \Delta q \quad (52)$$

where Δq is a small quantity (of order $\nabla T\ell$) to be determined. Substituting Eqs (51) and (52) into Eq (50) and neglecting the second order term yields:

$$(p_{UO_3})_{hot} - (p_{PuO_2})_{cold} = (1 - q_o)f'\nabla T\ell - f\Delta q \quad (53)$$

The subscript "cold" on f has been omitted, since this quantity may now be evaluated at the average pore temperature.

The first term on the right of Eq (53) is the temperature effect on the driving force at constant composition and the last term is the effect of composition difference across the pore at constant temperature.

In similar fashion, the equilibrium pressure of PuO_2 may be expressed by:

$$p_{PuO_2} = qh \quad (54)$$

where

$$h = \exp(-\Delta G^{\circ}_{vap,PuO_2}/RT) \tag{55}$$

and

$$\Delta G^{\circ}_{vap,PuO_2} = 136.4 - 35.9T \tag{56}$$

Treatment of the PuO_2 driving force in a manner analagous to that applied to UO_3 yields:

$$(p_{PuO_2})_{hot} - (p_{PuO_2})_{cold} = q_o h' \nabla T\ell + h\Delta q \tag{57}$$

where $h' = dh/dT$.

Substituting Eqs (53) and (57) into Eqs (48a) and (48b) and the results into Eq (47) permits Δq to be determined as:

$$\Delta q = \left[\frac{f' - h'}{\frac{f}{1-q_o} + \frac{h}{q_o}}\right] \nabla T\ell \tag{58}$$

The velocity of pore migration is given by:

$$v_p = \frac{J_{UO_3} + J_{PuO_2}}{N^{\circ}_U + N^{\circ}_{Pu}} \tag{59}$$

Using Δq of Eq (58) to determine the fluxes of the heavy metal oxides yields:

$$v_p = \frac{D\nabla T}{kT(N^{\circ}_U + N^{\circ}_{Pu})}\left[(1-q_o)f' + q_o h' - \frac{(f-h)(f'-h')}{\frac{f}{1-q_o} + \frac{h}{q_o}}\right] \tag{60}$$

The usual analyses of vapor transport in pores of pure UO_2 results in the velocity

$$(v_p)_{UO_2} = \frac{D\nabla T}{kTN^{\circ}_U} k' \tag{61}$$

where $k' = dk/dT$ and k is given by:

$$k = \exp(-\Delta G^{\circ}_{vap,UO_2}/RT) \tag{62}$$

where the free energy of UO_2 vaporization is given by Eq (26). The uranium concentration in pure UO_2 is approximately equal to the total heavy metal concentration in the mixed oxide. Division of Eq (60) by Eq (61) yields the ratio of the pore velocity in the mixed oxide to that in pure UO_2 at the same temperature and in the same temperature gradient:

$$\frac{v_p}{(v_p)_{UO_2}} = \frac{1}{k'}\left[(1-q_o)f' + q_o h' - \frac{(f-h)(f'-h')}{\frac{f}{1-q_o} + \frac{h}{q_o}}\right] \tag{63}$$

In the limit as $q_o \to 1$, the ratio of Eq (63) reduces to h'/k', which is the relative pore velocity in the two pure actinide oxides. As $q_o \to 0$, the ratio reduces to f'/k', which represents the rate of pore migration in hyperstoichiometric urania via UO_3 transport to that in stoichiometric uranium dioxide in which the diffusing species is UO_2. Because of the appreciable volatility of UO_3 in oxygen-rich urania, $(v_p)_{UO_{2+x}}/(v_p)_{UO_2}$ may be quite large.

For mixed oxides, a simpler form of Eq (63) may be obtained. Since the UO_3 pressure is very much larger than that of PuO_2 in hyperstoichiometric mixed oxide, the bracketed term in Eq (63) may be simplified by expanding using the conditions $f >> h$ and $f' >> h'$. This yields:

$$\frac{v_p}{(v_p)_{UO_2}} = \frac{h'}{k'} + \frac{hf'}{fk'}\left(\frac{1-q_o}{q_o}\right) \tag{64}$$

The thermochemical quantities in Eq (64) may be easily computed

for the pure oxides from Eqs (59) and (62). They are:

$$\frac{h'}{h} = \frac{135.5}{RT^2} \tag{65}$$

and

$$\frac{k'}{k} = \frac{136.4}{RT^2} \tag{66}$$

f' may be evaluated as follows. The uranium valence at the cold side of the pore is given by:

$$(V_U - 4)_{cold} = 2\left[\frac{(O/M)_o - 2}{1 - q_o}\right] \tag{67}$$

Equilibrium of the reaction $CO + 1/2O_2 = CO_2$ in the gas requires that

$$\Delta G°_C = -RT\ln(p_{CO_2}/p_{CO}) + \frac{1}{2}\Delta\bar{G}_{O_2} \tag{68}$$

where $\Delta G°_C$ is the standard free energy change of the CO_2/CO equilibrium, taken as $-67.5 + 20.75T$ and $\Delta\bar{G}_{O_2}$ is approximated by $-65 + 86(V_U-4)T$ for hyperstoichiometric mixed oxide. Using these formulas in Eq (68) and taking the derivative of the resulting equation with respect to T yields:

$$\frac{d(V_U-4)}{dT} = \frac{35}{43T^2} \tag{69}$$

Because the total carbon pressure in the gas has been assumed much larger than that of the other oxygen-bearing species, the CO_2/CO ratio is constant. Taking the derivative of f given by Eq (35) with respect to T and noting that C_1 and C_2 are functions of V_U only yields:

$$\frac{f}{f'} = \frac{1}{R}\left[\frac{dC_2}{d(V_U-4)} - \frac{1}{T}\,\frac{dC_1}{d(V_U-4)}\right]\frac{d(V_U-4)}{dT} + \frac{C_1}{RT^2} \qquad (70)$$

Substitution of Eqs (36) and (69) into Eq (70) gives:

$$\frac{f'}{f} = \frac{35\left[1-\frac{1}{2}(V_U-4)\right] + C_1}{RT^2} \qquad (71)$$

Application of Eq (64) to a mixed oxide containing 20% Pu shows that pore migration is approximately three times faster than in pure UO_2. This ratio is only slightly affected by temperature in the range 1500°K to 2500°K and oxygen-to-metal ratios from 2.02 to 2.05. This factor of 3 increase is in qualitative agreement with observation of pore migration velocities in mixed oxides (22).

Since the plutonium fraction at the hot surface of the pore is greater than that of the virgin fuel, a plutonium concentration profile precedes the moving pore. The plutonium concentration ahead of the pore may be expressed by:

$$N_{Pu} = N^{\circ}_{Pu} q/q_o \qquad (72)$$

If we take a reference frame moving with the pore, the diffusion equation for plutonium in the solid is:

$$v_p \frac{dq}{dz} + D_s \frac{d^2q}{dz^2} = 0 \qquad (73)$$

where z is the distance into the solid from the hot face of the pore and D_s is the diffusion coefficient of plutonium in the mixed oxide. The boundary condition on Eq (73) at z = 0 is given by Eq (58) and as $z\to\infty$, $q\to q_o$. The solution is:

$$q-q_o = \Delta q \exp\left(-\frac{v_p}{D_s} z\right) \qquad (74)$$

Since D_s/v_p is small ($\sim 10^{-5}$cm at 2000°K), the perturbation of the solid composition extends only a very small distance in front of the moving pore. Figure 12 shows an exaggerated sketch of the plutonium profile in front of the pore.

V. SUMMARY

The two geometries by which actinide vapor migration by gas phase diffusion alters fuel properties act in complementary ways.

Continuous cracks or fissures along the temperature gradient are ineffective in restructuring but are quite suitable for actinide redistribution. To avoid self-termination of the process due to crack closure by condensing vapors, mechanical processes must continually operate to open healed cracks or to create new ones.

Closed pores migrating up the temperature gradient, on the other hand, provide an efficient means of fuel restructuring but do not contribute to actinide redistribution. A lenticular pore passing through a mixed oxide fuel body is much like a wrinkle in a rug or a dislocation in a crystal. Once the disturbance has passed, the medium returns to its normal state except for gross displacement by an amount equal to the dimension of the disturbance.

Acknowledgement This work was carried out under the auspices of the U. S. Atomic Energy Commission.

TABLE 1

Uranium Redistribution Characteristics in 20% Plutonium Mixed Oxide Fuels

Symbol	b/L	$(O/M)_o$	T_o, °K	T_s, °K	p_C, atm	$p^*(0,0)$, atm[a]	τ, hr[b]	$t_{\frac{1}{2}}$ at $t/\tau = 15$, hr
A	0.1	2.05	2500	1000	1	6.8×10^{-2}	2.2	c
B	0.01	2.05	2500	1000	1	6.8×10^{-2}	2.2	350
C	0.1	2.02	2500	1000	1	1.6×10^{-2}	9.4	1160
D	0.1	2.05	2500	1500	1	4.2×10^{-2}	3.6	260

a calculated by Eq (29) with $\gamma_U = 1.0$, $T = T_o$ and $\Delta\bar{G}_{O_2}$ and V_U at $Z = 0$ after oxygen redistribution.

b for L=0.2 cm, H=0.1 cm, D=0.2 cm^2/sec at 2000°K, $N_U^\circ = 2.0 \times 10^{22}$ atoms/cn^3

c calculation unstable for $t/\tau > 12$.

LITERATURE CITATIONS

1. P. E. Novak, T. A. Lauritzen, R. Protsik, J. H. Davies and E. L. Zebroski, ANL-7120, pp. 392-399 (1965).

2. E. A. Aitken, and S. K. Evans, Plutonium 1970, Proc. of the Fourth Int'l Conf. on Plutonium and Other Actinides, Nuclear Metallurgy, Vol. 17, Part II, p. 772, The Metallurgical Society of the AIME (1970).

3. M. G. Chasanov and D. F. Fischer, ANL-7703 (1970).

4. M. G. Adamson and E. A. Aitken, Trans. Amer. Nucl. Soc., 14, 179 (1971).

5. M. Bober, C. Sari, and G. Schumacher, Trans. Amer. Nucl. Soc., 12, 603 (1969).

6. J. K. Bahl, and M. D. Freshley, Trans. Amer. Nucl. Soc., 13, 599 (1970).

7. A. R. Olsen, R. B. Fitts, and W. J. Lackey, Proc. of Conf. on Fast Reactor Fuel Element Technology, p. 579, New Orleans, Amer. Nucl. Soc. (1971).

8. M. Bober, C. Sari, and G. Schumacher, J. Nucl. Mater. 40, 341 (1971).

9. R. O. Meyer, D. R. O'Boyle and R. Natesh, Trans. Amer. Nucl. Soc., 14, 182 (1971).

10. R. O. Meyer, E. M. Butler, and D. R. O'Boyle, Trans. Amer. Nucl. Soc., 15, 216 (1972).

11. D. R. De Halas and G. R. Horn, J. Nucl. Mater. 8, 207 (1963).

12. M. V. Speight, J. Nucl. Mater. 13, 207 (1964).

13. R. S. Barnes and R. S. Nelson, AIME Nucl. Met. Symp. of Radiation Effects in Solids, Asheville, N. C. (1965).

14. F. A. Nichols, J. Nucl. Mater. 27, 137 (1968); ibid. 30, 143 (1969).

15. R. W. Weeks, R. O. Scattergood and S. R. Pati, J. Nucl. Mater., 36, 223 (1970).

16. M. H. Rand and T. L. Markin, IAEA Symp. on Thermodynamics of Nuclear Materials, p. 637, Vienna (1967).

17. H. S. Carslaw and J. C. Jaeger, Conduction of Heat in Solids, p. 167, Second Edition, Oxford (1959).

LITERATURE CITATIONS Cont.

18. D. R. Olander, J. Nucl. Mater., to be published.

19. W. Oldfield and J. B. Brown, Jr., Mater. Sci. Eng., 6, 361 (1970).

20. H. Beisswenger, M. Bober and G. Schumacher, Proc. of Symp. on Plutonium as a Reactor Fuel, p. 273-282, Brussels, IAEA (1967).

21. W. G. Pfann, Trans. AIME 194, 747 (1952).

22. L. C. Michels, R. B. Poeppel and L. A. Neimark, Trans. Amer. Nucl. Soc. 13, 601 (1970).

FIGURE CAPTIONS

1. Model of a fuel piece with a crack along the temperature gradient.

2. Normalized partial pressure profiles in a crack. UO_2 transport, b/L = 0.2.

3. Dimensionless flux of UO_2 at the crack surface.

4. Integral of the absolute flux, UO_2 transport.

5. Flow diagram for computations of uranium transport in mixed oxide fuel.

6. Normalized UO_3 and PuO_2 pressures at the crack surface. Conditions listed in text.

7. Dimensionless flux of UO_3 at crack surface. Conditions listed in text.

8. Fuel composition profiles for various times of redistribution. Conditions listed in text.

9. Profiles of oxygen potential and uranium valence during redistribution. Conditions listed in text.

10. Profiles of the CO_2/CO ratio during redistribution. Conditions listed in text.

11. Extent of uranium redistribution as a function of dimensionless time. Symbols on curves described in Table 1.

12. A migrating lenticular pore in mixed oxide fuel.

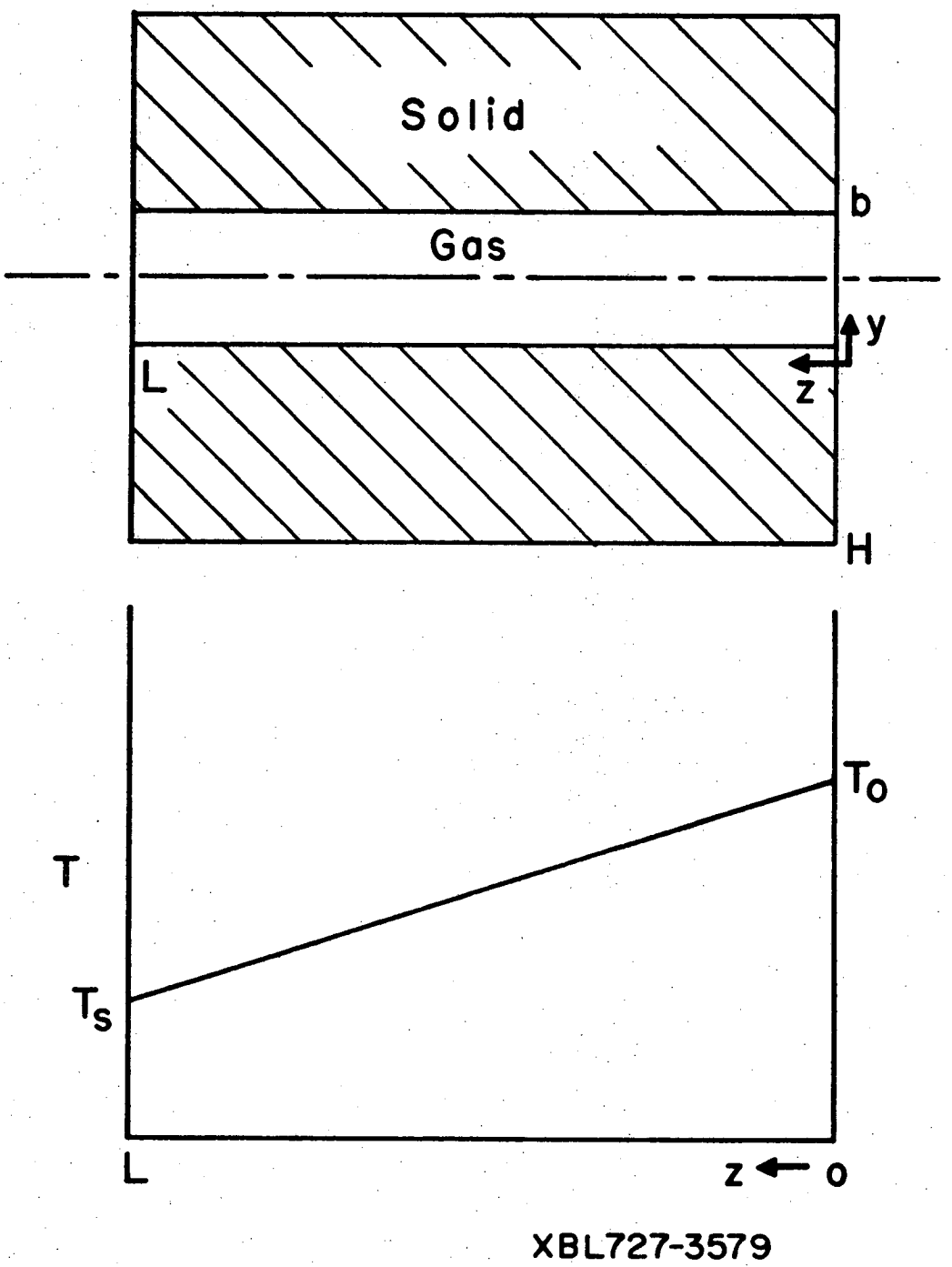

Fig. 1

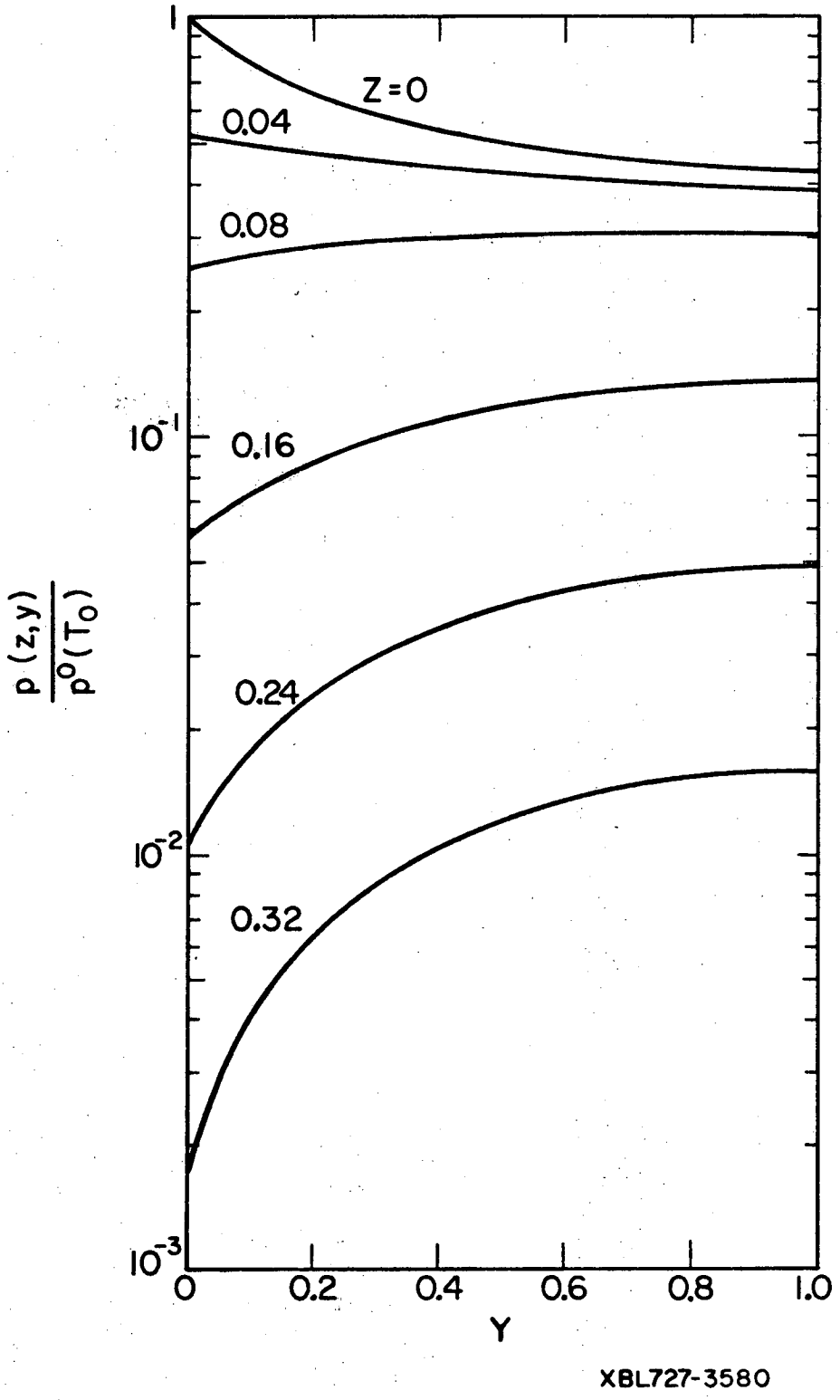
1
Z=0
0.04
0.08
10^{-1}
0.16
0.24
10^{-2}
0.32
10^{-3}
0
0.2
0.4
0.6
0.8
1.0
Y
$\frac{p(z,y)}{p^0(T_0)}$
XBL727-3580

Fig. 2

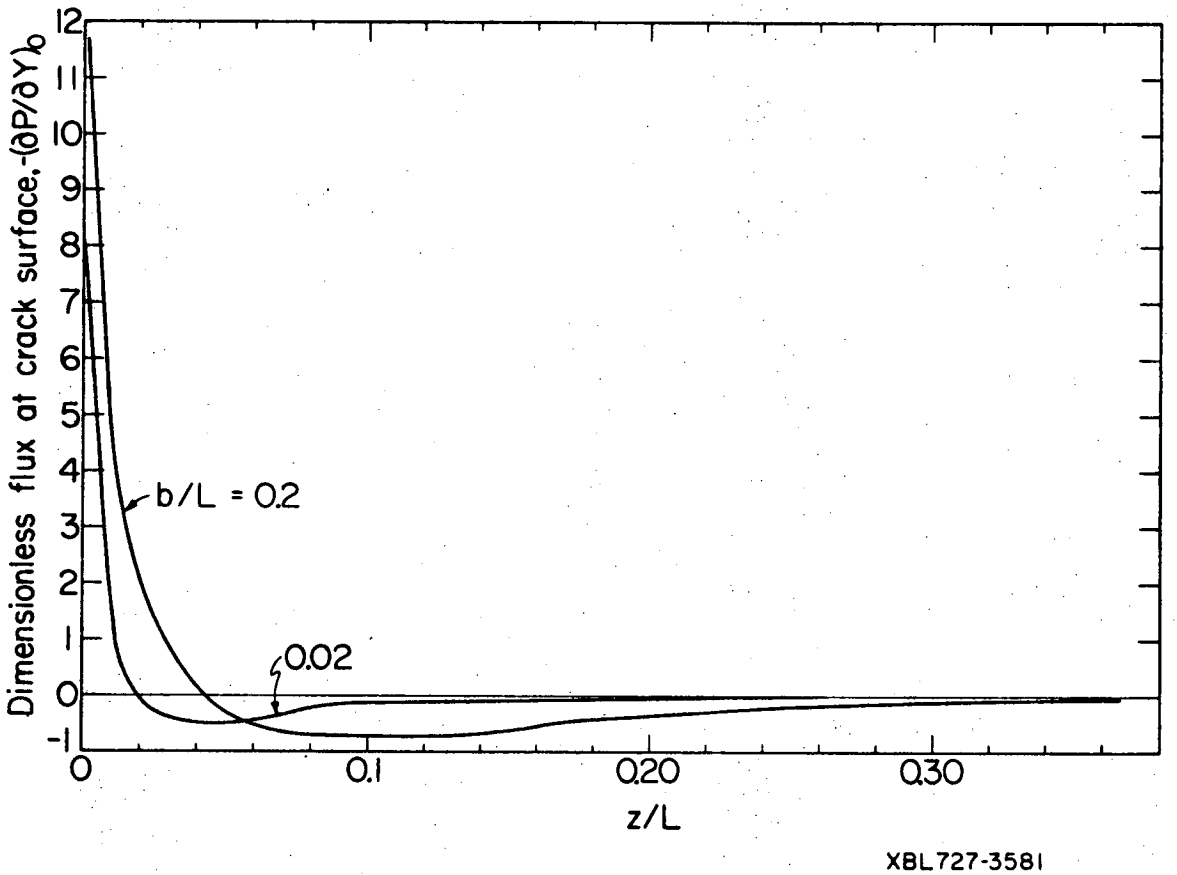
Dimensionless flux at crack surface, $-(\partial P/\partial Y)_0$
12
11
10
9
8
7
6
5
4
3
2
1
0
-1
b/L = 0.2
0.02
0
0.1
0.20
0.30
z/L
XBL727-3581

Fig. 3

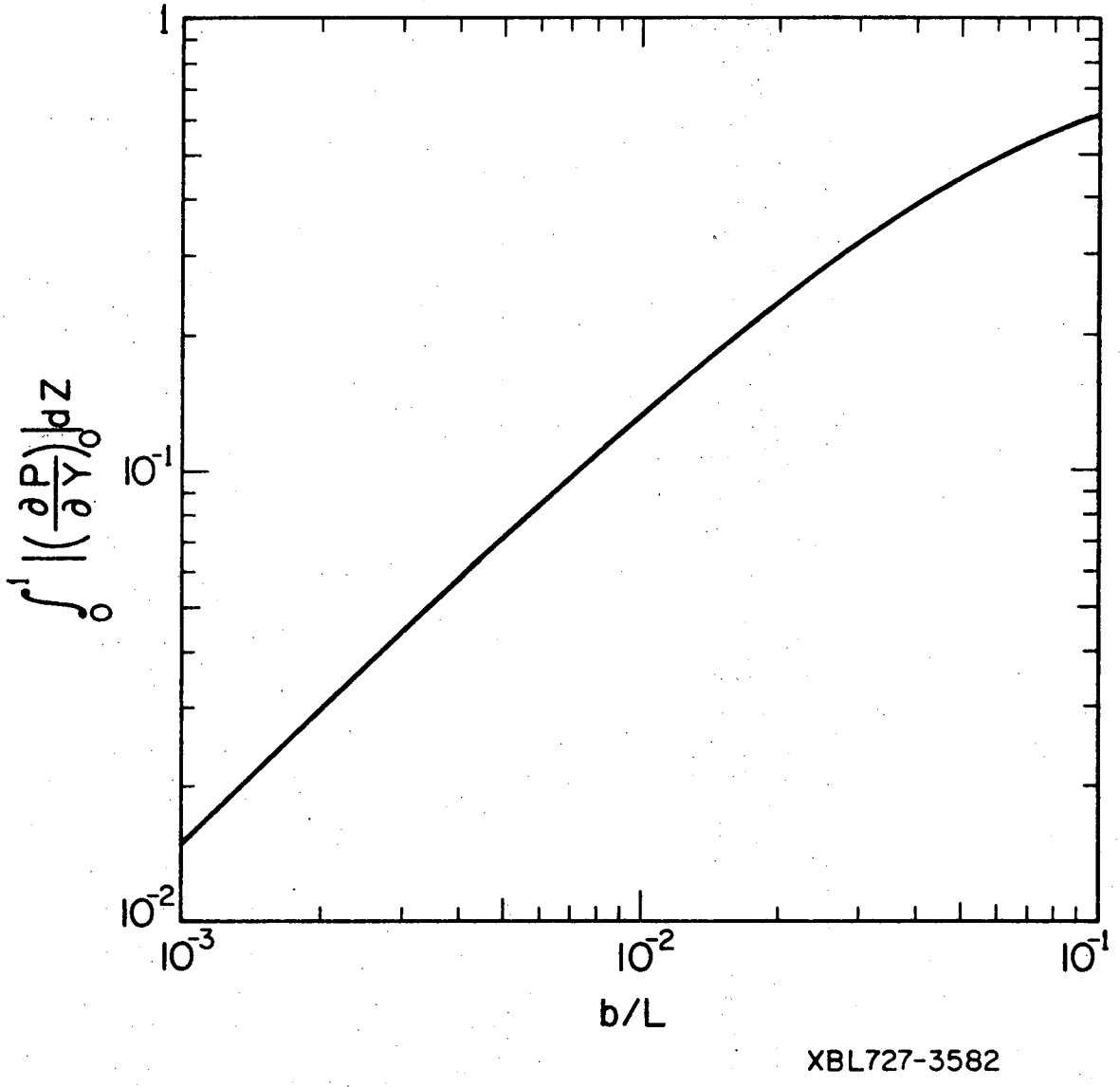

Fig. 4

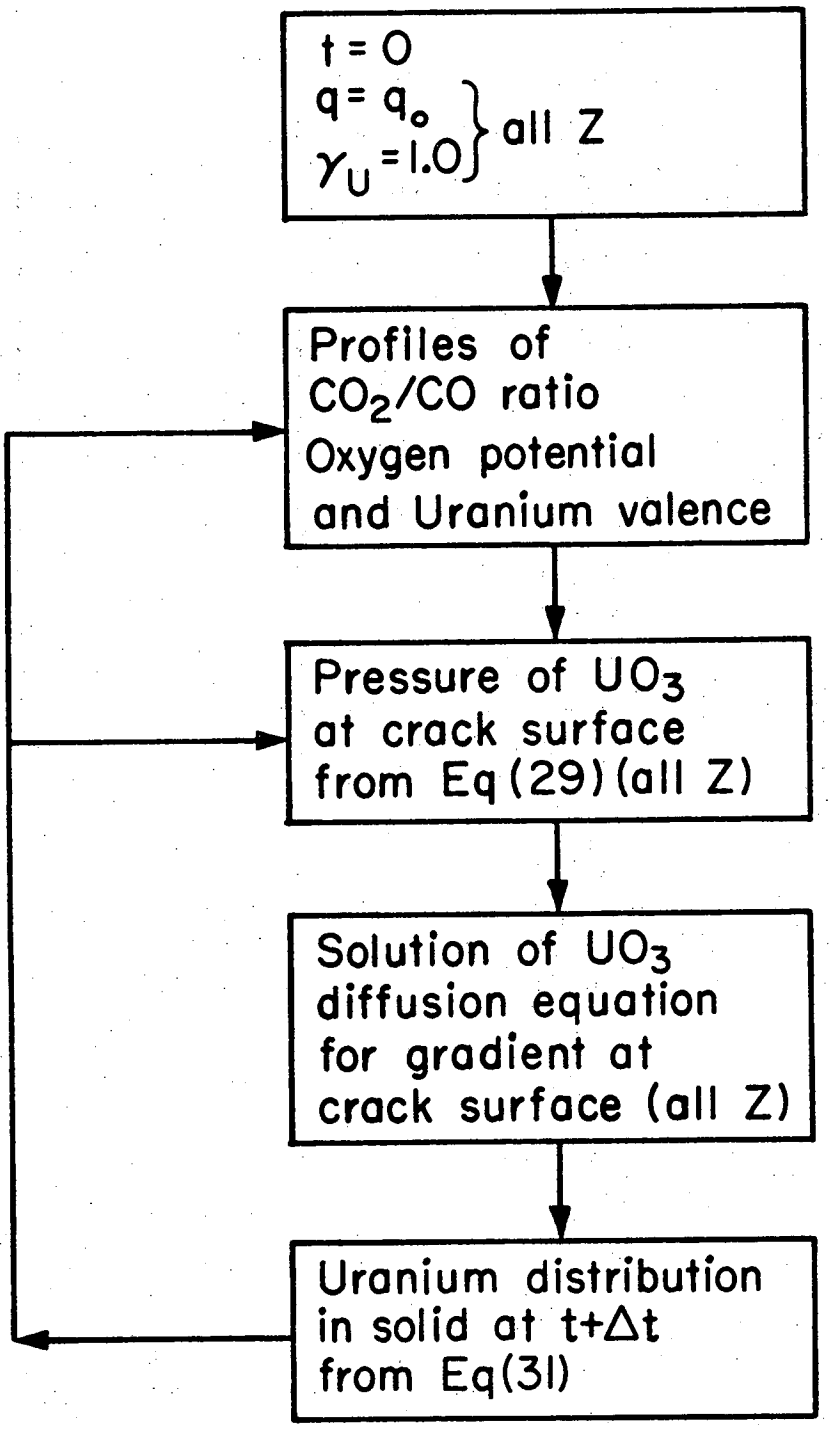

XBL727-3583

Fig. 5

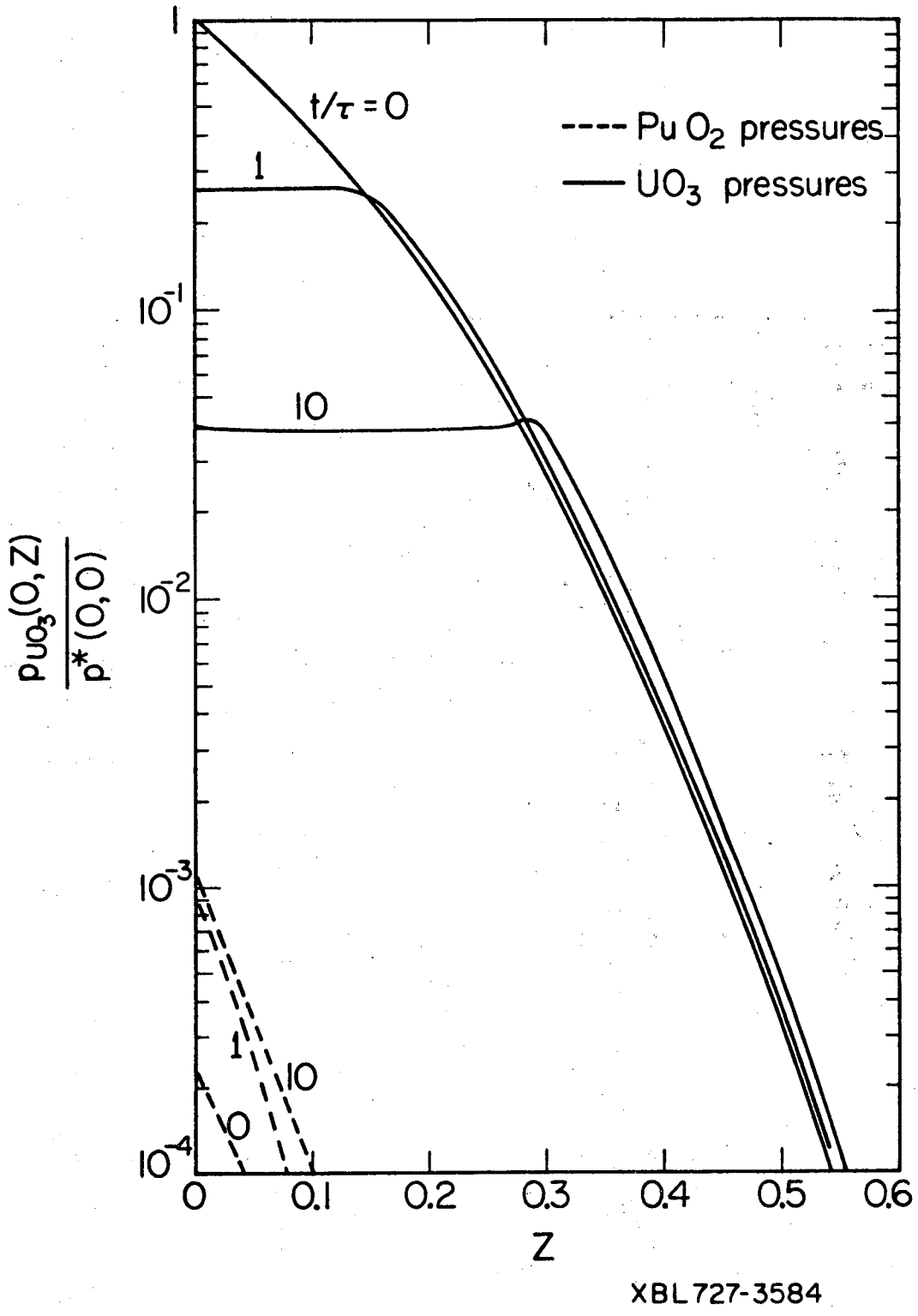
1
10^{-1}
10^{-2}
10^{-3}
10^{-4}
$\frac{p_{UO_3}(0,Z)}{p^*(0,0)}$
$t/\tau = 0$
1
10
0
1
10
---- PuO_2 pressures
—— UO_3 pressures
0
0.1
0.2
0.3
0.4
0.5
0.6
Z
XBL727-3584

Fig. 6

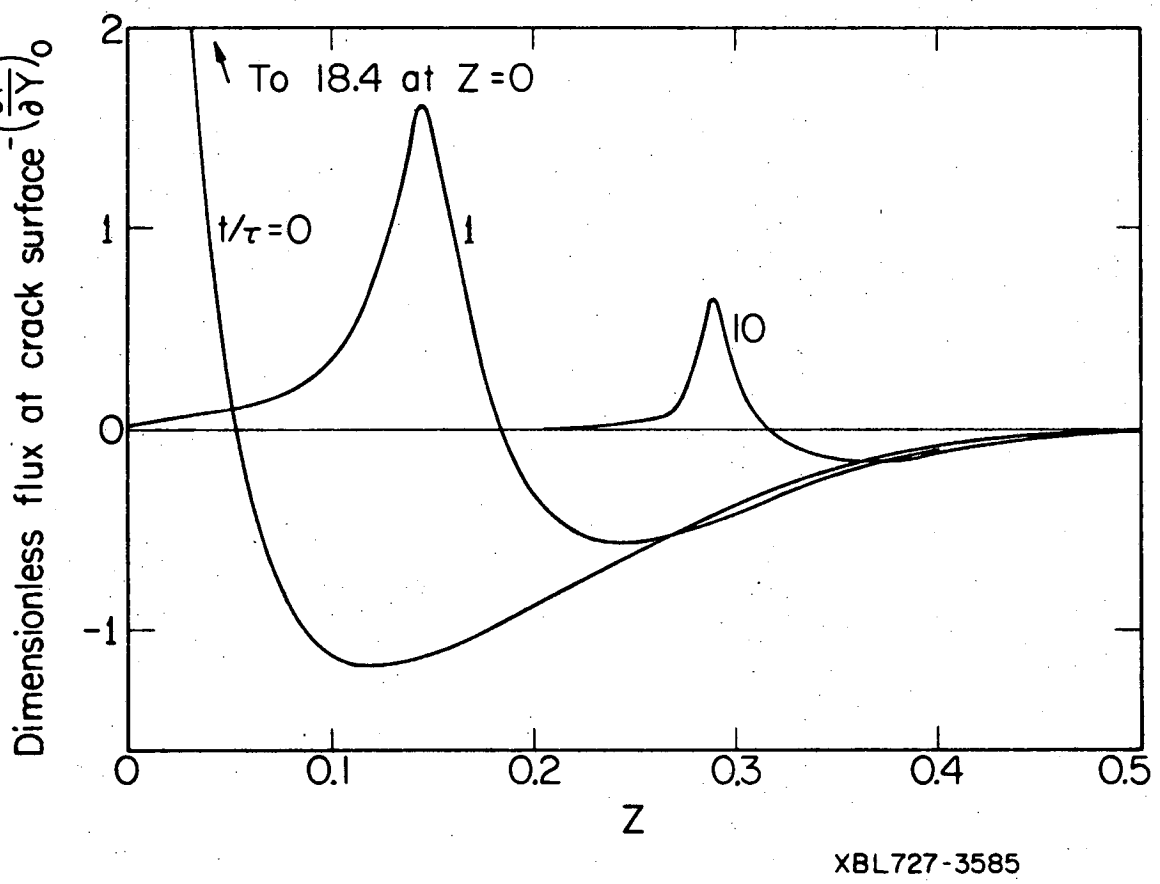
Dimensionless flux at crack surface $-\left(\frac{\partial P}{\partial Y}\right)_0$
To 18.4 at Z=0
t/τ=0
1
10
2
1
0
-1
0
0.1
0.2
0.3
0.4
0.5
Z
XBL727-3585

Fig. 7

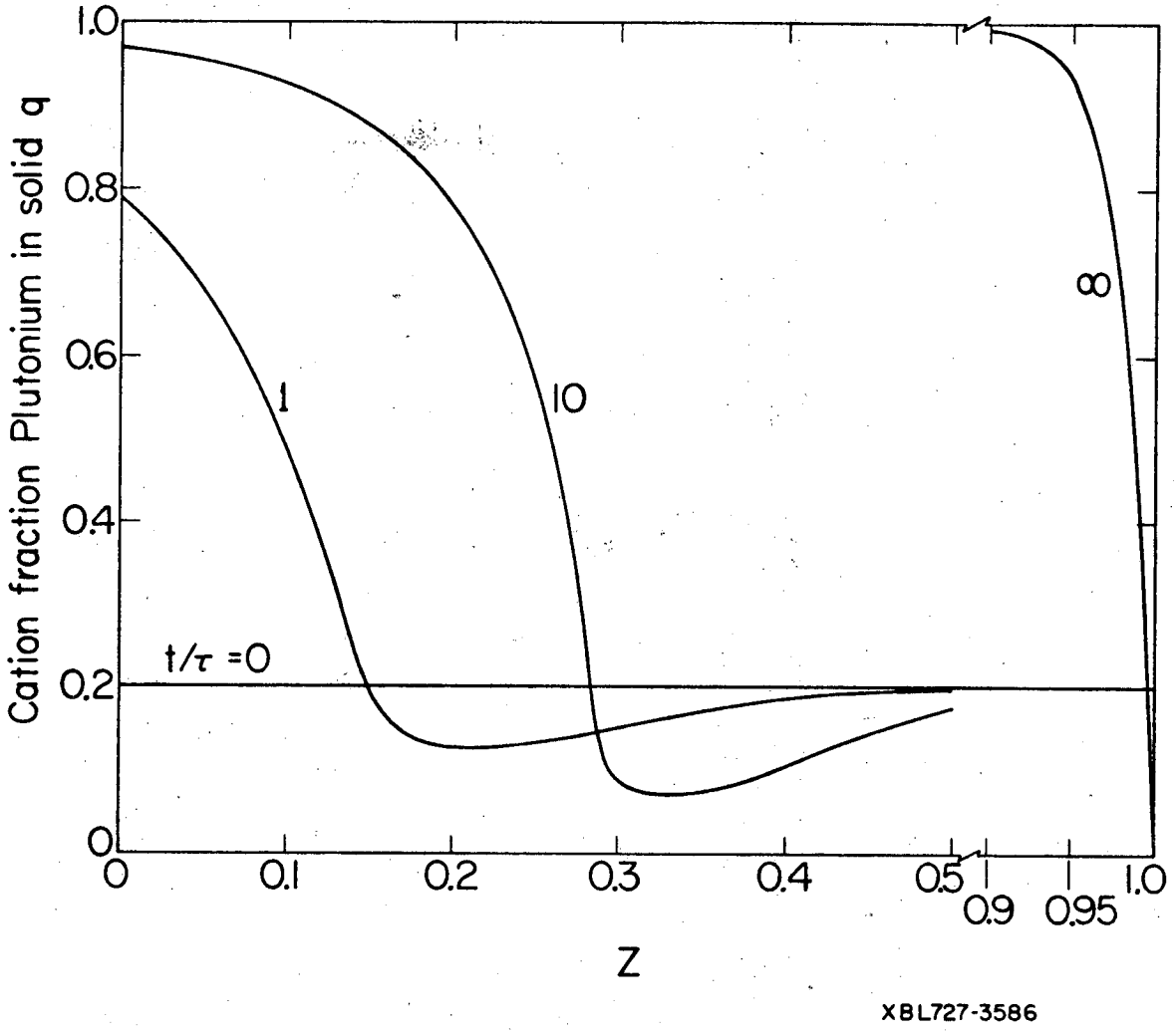

Fig. 8

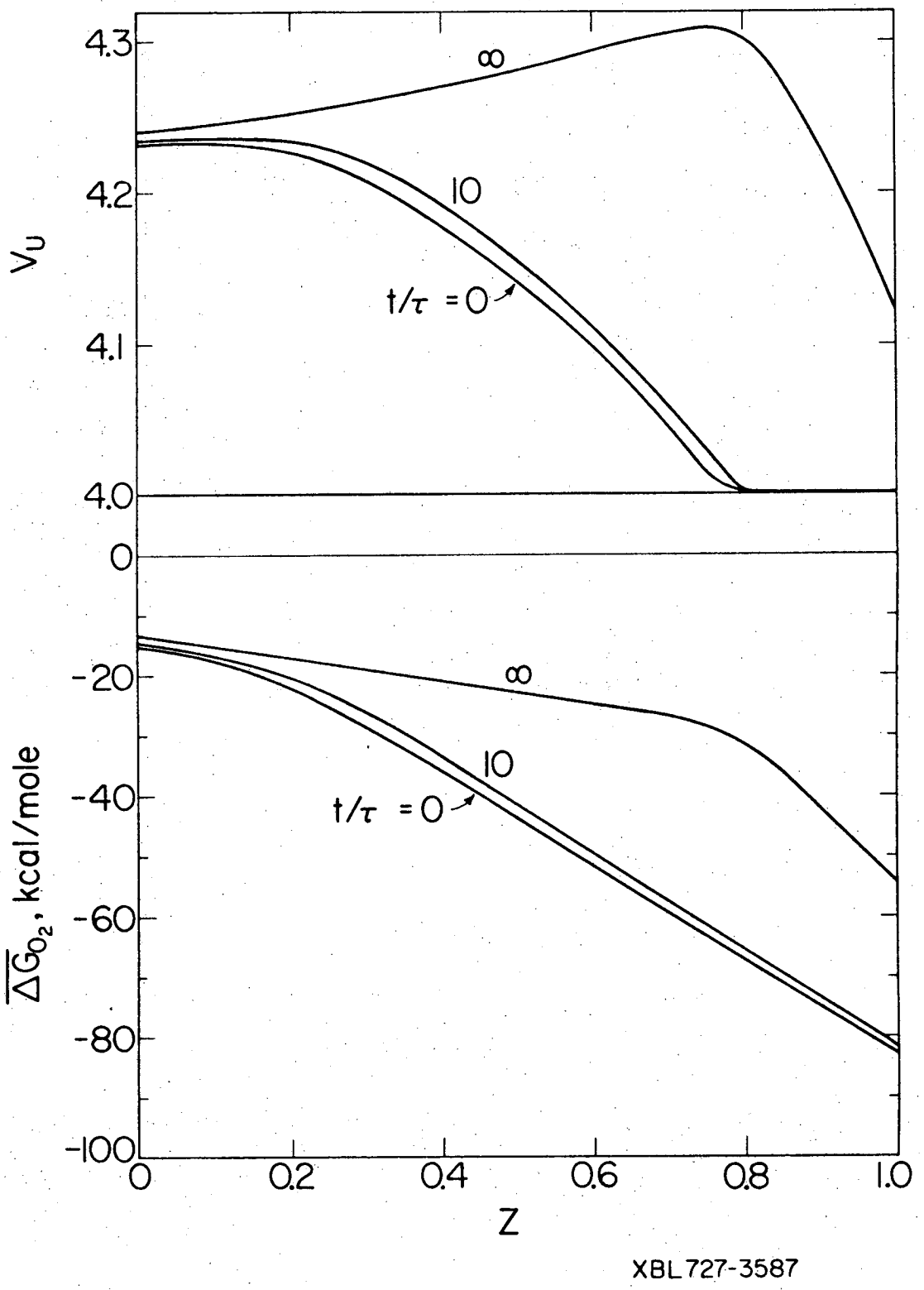
4.3
4.2
4.1
4.0
V_U
∞
10
t/τ = 0
0
-20
-40
-60
-80
-100
$\overline{\Delta G}_{O_2}$, kcal/mole
∞
10
t/τ = 0
0
0.2
0.4
0.6
0.8
1.0
Z
XBL727-3587

Fig. 9

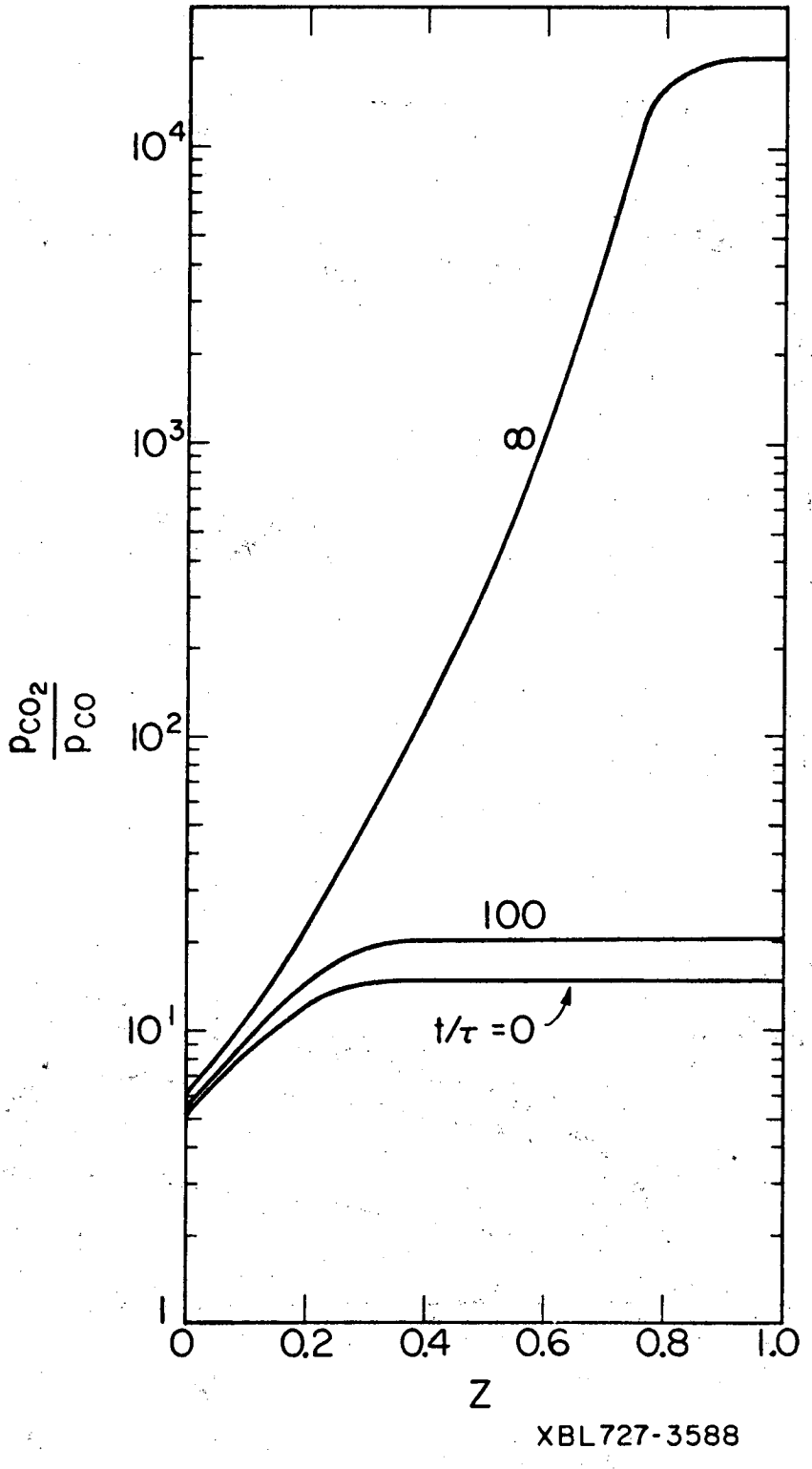

Fig. 10

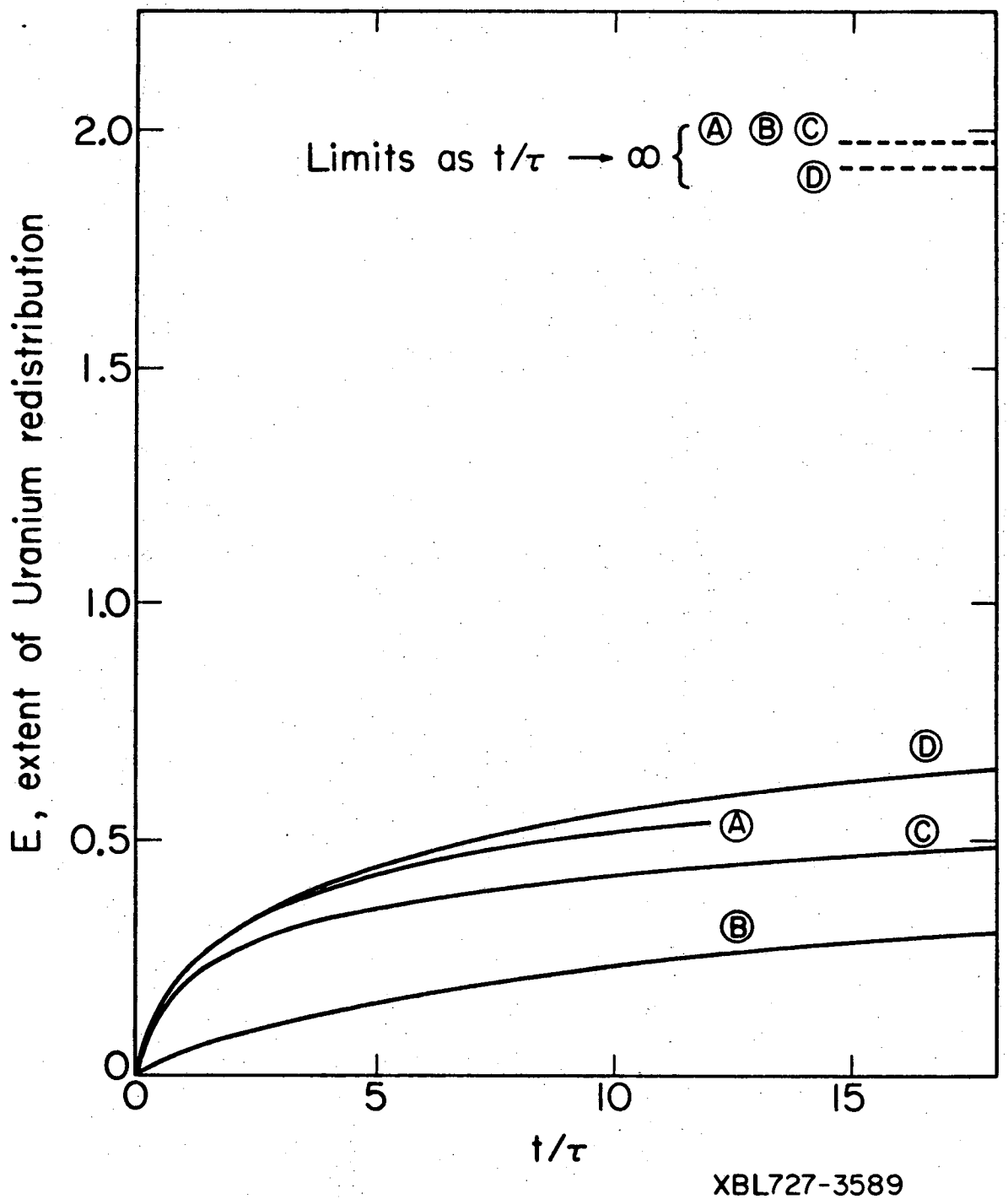
Limits as t/τ → ∞ { Ⓐ Ⓑ Ⓒ Ⓓ
2.0
1.5
1.0
0.5
0
E, extent of Uranium redistribution
0
5
10
15
t/τ
Ⓓ
Ⓐ
Ⓒ
Ⓑ
XBL727-3589

Fig. 11

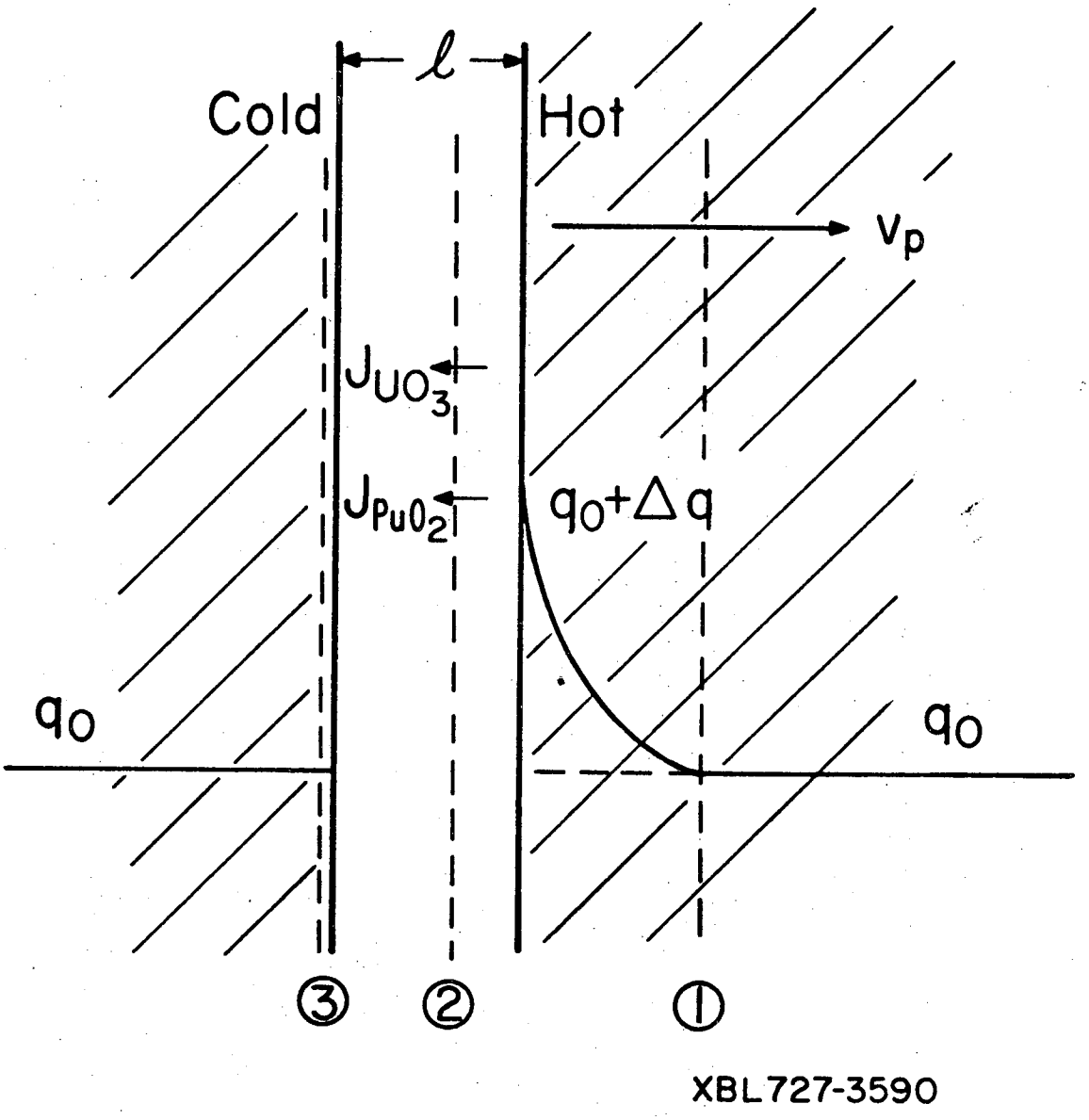

Fig. 12

TECHNICAL INFORMATION DIVISION
LAWRENCE BERKELEY LABORATORY
UNIVERSITY OF CALIFORNIA
BERKELEY, CALIFORNIA 94720